INSTITUTE OF PHYSICS PUBLISHING JOURNAL OF PHYSICS D: APPLIED PHYSICS
J. Phys. D: Appl. Phys. **37** (2004) 240–248 PII: S0022-3727(04)66583-1

Morphological stability in epitaxially strained films on a substrate with finite thickness

Jian-Ming Lu[1], **Ming-Horng Su**[2], **Jee-Gong Chang**[3] **and Chi-Chuan Hwang**[1,4]

[1] Department of Engineering Science, National Cheng Kung University, Tainan, Taiwan, Republic of China
[2] Department of Fire Science, Wufeng Institute of Technology, Chiayi, Taiwan, Republic of China
[3] National Center for High-Performance Computing, No 21, Nan-Ke 3rd Road, Hsin-Shi, Tainan, Taiwan, Republic of China

E-mail: chchwang@mail.ncku.edu.tw

Received 29 July 2003
Published 19 December 2003
Online at stacks.iop.org/JPhysD/37/240 (DOI: 10.1088/0022-3727/37/2/012)

Abstract
This paper investigates the morphological stability of epitaxial films growing heteroepitaxially on ultra-thin substrates. The misfitting strain model is incorporated into the quasi-static mechanical equilibrium system. The interfacial evolution equation between the vapour and film phases is used to solve the film evolution. The perturbation method of normal modes is used to derive the analytical form of the normal-mode growth rate. Additionally, this paper investigates the dynamic behaviour of the vapour–film interface. The results of the study show that a decrease in substrate thickness tends to stabilize the system regardless of whether the stiffness ratio, ρ (i.e. the ratio of film stiffness to substrate stiffness) is less than, equal to or greater than unity. Furthermore, it is found that the effects of a finite substrate thickness on the stability behaviour of the system are quite profound, and that this is particularly true when the film thickness is close to h_c with values of stiffness ratio greater than unity.

1. Introduction

Applications of the ultra-thin wafer have now become widespread with the development of more complex miniaturized systems, which facilitate much denser three-dimensional packaging [1]. Utilization of ultra-thin wafers is beneficial since it improves certain operating properties, including electronic properties [2, 3], mechanical properties [4, 5] and thermal properties [5]. In research conducted by Sriram and Smith [2], it was noted that these properties are significantly influenced by the thickness of the substrate. It is well-known that different morphologies are formed during the growth of epitaxially deposited films on a substrate, and that the transition of these morphologies is largely dependent upon the presence of elastic stress and stress-relieving misfit dislocations [6–8]. Furthermore, it can be demonstrated that as the substrate thickness decreases, the coupling of stress states between the film and the substrate induced by lattice mismatches assumes a more dominant influence. Clearly, therefore, it is essential to develop an understanding of the morphological instability induced by misfitting strain for ultra-thin substrates.

The subject of stress-driven, morphological stability was originally investigated by Asaro and Tiller [9]. In their study of stress corrosion cracking of an elastic solid, they proposed the use of the chemical potential to derive an evolution equation of the solid surface, which took into account the effects of the surface energy and the strain energy. Srolovitz [10] studied the surface stability of stressed solids. In his investigation, the surface evolution equation taken considered the effects of evaporation/condensation and surface diffusion. Previously, the instability of the interface between the two phases had been investigated by considering the stress states of the film phase

[4] Author to whom any correspondence should be addressed.

and the substrate phase separately. Grinfel'd [11] analysed the second variation of energy in his theoretical study of the instability of the separation boundary between a non-hydrostatically stressed elastic body and a melt. Spencer *et al* [6–8] investigated the stability of the vapour–film interface, and focused particularly upon the role of misfitting strain in inducing interface instability. In other words, the stress states of the two phases, i.e. the film and the substrate, were considered together. Junqua and Grillhé [12] used the two-phase model and the surface dislocation model to investigate the instability of epitaxial films in the case of sinusoidal roughness at the film surface. Gao [13] studied the interface instability for different surface morphologies, namely cusp-like, cracked and flat surface geometries. Although all of the studies mentioned above provided a profound contribution to the understanding of surface instability under different circumstances, they all considered a substrate of infinite thickness. In the study performed by Ma *et al* [4], relating to applications of ultra-thin substrates, the ratio of film thickness (500 nm) to substrate thickness (25 μm) is very small. Hence, it is necessary to consider a substrate of finite thickness.

The objective of this current study is to investigate the morphological stability of an epitaxially strained film growing heteroepitaxially or homoepitaxially on an ultra-thin substrate. The misfitting strain, which arises due to differences between the lattice constants of the film and the substrate, is incorporated into the quasi-static mechanical equilibrium system, and the interfacial evolution equation between the vapour and the solid phases is established. The perturbation method of normal modes is employed to generate the dynamic behaviour of the vapour–film interface. The closed form solution of the normal-mode growth rate, and the critical film thickness, h_c, are both obtained. Finally, this paper describes and discusses the influence of a finite substrate thickness on the stability characteristics of the system.

2. Mathematical formulation

The isotropic linear elastic, quasi-static model, consisting of the film and the substrate, is presented in figure 1. As stated previously, the misfitting strain model is applied to the film–substrate interface. The associated boundary conditions are formulated, and the time dependent interface between the vapour and the film is modelled by using an evolution equation, which takes into account the effects of vapour deposition and surface diffusion.

2.1. Governing equations

(1) Strain–displacement relation:

$$E_{ij} = \tfrac{1}{2}(\partial_j u_i + \partial_i u_j) \tag{1}$$

where E_{ij} is the strain tensor and u_i is the displacement component.

(2) Constitutive equations:

(i) for the film:

$$T^{\mathrm{F}}_{ij} = 2\mu^{\mathrm{F}}\left[\left(\frac{\nu^{\mathrm{F}}}{1-2\nu^{\mathrm{F}}}\right)\delta_{ij}E^{\mathrm{F}}_{kk} + E^{\mathrm{F}}_{ij} - \left(\frac{1+\nu^{\mathrm{F}}}{1-2\nu^{\mathrm{F}}}\right)\varepsilon\delta_{ij}\right]. \tag{2}$$

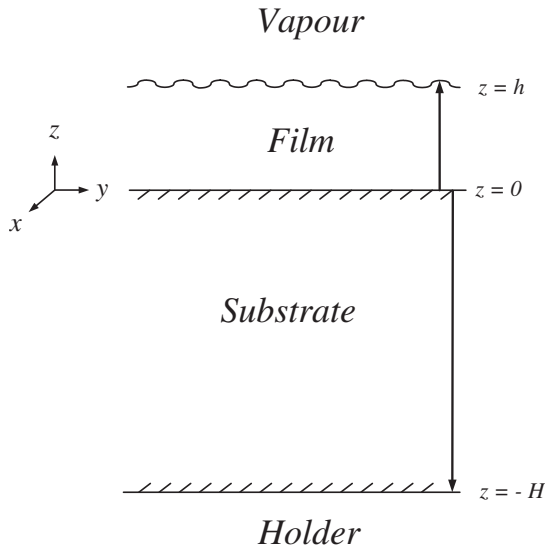

Figure 1. Physical configuration.

(ii) for the substrate:

$$T^{\mathrm{S}}_{ij} = 2\mu^{\mathrm{S}}\left[\left(\frac{\nu^{\mathrm{S}}}{1-2\nu^{\mathrm{S}}}\right)\delta_{ij}E^{\mathrm{S}}_{kk} + E^{\mathrm{S}}_{ij}\right]. \tag{3}$$

In these two equations, T_{ij} is the stress tensor; μ the shear modulus; ν the Poission ratio; and δ_{ij} is the Kronecker delta. The superscripts F and S refer to the film and substrate phases, respectively.

The presence of an extra term in equation (2), compared to equation (3), is to be noted. This term arises from the misfitting strain induced by lattice mismatches between the film and the substrate. The misfitting strain is given by

$$\varepsilon = \frac{a_{\mathrm{F}} - a_{\mathrm{S}}}{a_{\mathrm{S}}} \tag{4}$$

where a_{F} and a_{S} are the lattice constants of the film and substrate, respectively.

(3) Mechanical equilibrium equation. The film and the substrate are both satisfied by the following equilibrium equation:

$$\partial_j T_{ij} = 0. \tag{5}$$

(4) Displacement equilibrium equation. The equilibrium equation can be expressed in terms of displacement by substituting the constitutive equations (1) and (2) into (5), and then replacing the strain components with corresponding displacement elements by means of the strain–displacement relationship. The resulting equation is as follows:

$$(1-2\nu)\partial_k^2 u_i + \partial_i\partial_k u_k = 0. \tag{6}$$

It is to be noted that this equation is valid for both the film and the substrate.

2.2. Boundary condition

A traction-free boundary condition is imposed at the upper interface of the film. This simulates the condition where the pressure of the surrounding vapour is very low, i.e.

$$T^{\mathrm{F}}_{ij} n^{\mathrm{F}}_j = 0 \qquad \text{on } z = h \tag{7}$$

where $z = h(x, y, t)$ is the time-varying film thickness; and n_j represents the unit normal to the film–vapour surface oriented toward the vapour.

The continuity conditions of displacement and stress are applied at the film–substrate interface, i.e.

$$u_i^{\mathrm{F}} = u_i^{\mathrm{S}}, \quad T_{3i}^{\mathrm{F}} = T_{3i}^{\mathrm{S}} \qquad \text{on } z = 0. \tag{8}$$

At the substrate–holder interface, the imposed boundary condition must reflect the clamping situation which is actually applied in practice. Within semiconductor manufacturing, several methods exist for the clamping of the substrate to the holder. These methods include the magnetic chuck, the electrostatic chuck (E-chuck), the vacuum chuck and the rinse/dryer chuck. Depending upon the particular method employed, the attractive forces exerted between the substrate and the holder may be produced by a magnetic force, an electrostatic force, or a combined vacuum and mechanical clamping force. The objective of the chuck force is to prevent the substrate from shifting or deforming. This enables a more precise manufacturing operation which yields improved film properties during the exposure and deposition stages. In order to prevent the substrate from shifting or deforming, the material used for the holder must be stiffer than the material used for the substrate. Hence, the deformation of the holder will be relatively smaller than that of the substrate, and this enables the assumption to be made that the holder is rigid. Therefore, the displacement of the substrate base, which is the closest substrate layer to the top of the holder, can be specified as being equal to zero, i.e. a zero displacement boundary condition is imposed at the substrate–holder interface. This condition assumes that the substrate is perfectly attached to the holder, and that the holder is perfectly rigid in comparison to the stiffness of the non-deformed substrate, i.e.

$$u_i^{\mathrm{S}} = 0 \qquad \text{on } z = -H. \tag{9}$$

The equations given above form a closed system which can be used to solve a quasi-static equilibrium problem, and which are used in this case to derive the basic state solution component of the stability analysis. In order to investigate the morphological instability of the film surface, it is necessary to consider the evolution equation of the film surface.

The general evolution equation is derived from the chemical potential [7, 8], and chiefly focuses upon the physical mechanisms of surface diffusion and vapour deposition in the evolution of the film. The simplified evolution equation is given as:

$$\frac{\partial h}{\partial t} = D(1 + |\nabla h|^2)^{1/2}\nabla_{\mathrm{S}}^2 (E + \gamma K) + V \qquad \text{on } z = h(x, y, t) \tag{10}$$

where ∇ is the gradient operator; ∇_{S}^2 the surface Laplacian operator; $|\nabla h|^2 = h_x^2 + h_y^2$; D the surface diffusivity, which is dependent upon temperature; $E(= (E_{ij} - \varepsilon\delta_{ij})T_{ij}/2)$ the elastic strain energy density; γ the surface free energy of the film; K the curvature of the film surface; and V is the deposition rate of the vapour. It is noted that the value of K used in the simulation is taken to be the measurement at atmospheric pressure for the purposes of simplicity [7, 8]. Since the temperature difference throughout the whole system is small, a constant temperature is assumed, and as a consequence, a constant value of surface diffusivity, D, is adopted.

3. Linear stability analysis

3.1. Basic state solutions

The film evolution given in equation (10) can be solved for either the static or the dynamic case, depending upon the form of the film thickness expression. In this study, only the static film solution is considered, and hence the film thickness is expressed as:

$$\bar{h} = h_0 \tag{11}$$

where $\bar{h}$ represents the basic state solution of the static film.

The displacement field of the substrate corresponding to the condition of zero strain is given as:

$$\bar{u}_i^{\mathrm{S}} = 0 \qquad \text{for } i = 1, 2, 3. \tag{12}$$

The displacement field corresponding to a state of uniform epitaxial strain in the z-direction is expressed as:

$$\bar{u}_i^{\mathrm{F}} = 0 \quad \text{for } i = 1, 2, \qquad \text{and} \qquad \bar{u}_3^{\mathrm{F}} = E_{33}^0 z \tag{13}$$

where

$$E_{33}^0 = \varepsilon\left[\frac{1 + \nu^{\mathrm{F}}}{1 - \nu^{\mathrm{F}}}\right].$$

The biaxial stress associated with the strain fields in the film is:

$$\bar{T}_{11}^{\mathrm{F}} = \bar{T}_{22}^{\mathrm{F}} = -2\mu^{\mathrm{F}} E_{33}^0 = -2\mu^{\mathrm{F}}\varepsilon\left[\frac{1 + \nu^{\mathrm{F}}}{1 - \nu^{\mathrm{F}}}\right]. \tag{14}$$

3.2. Normal-mode perturbation

The perturbation method of the normal modes is employed to study the linear stability of the strained film. The perturbation is superimposed on the planar shape of the free surface obtained from the basic solution. The perturbed solutions are expressed as:

$$h = \bar{h}(t) + \hat{h}(t)\phi(x, y) \tag{15}$$

$$u_i^{\mathrm{S}} = 0 + \hat{u}_i^{\mathrm{S}}(z, t)\phi(x, y) \qquad \text{for } i = 1, 2, 3 \tag{16}$$

$$u_i^{\mathrm{F}} = 0 + \hat{u}_i^{\mathrm{F}}(z, t)\phi(x, y) \qquad \text{for } i = 1, 2 \tag{17}$$

$$u_3^{\mathrm{F}} = E_{33}^0 z + \hat{u}_3^{\mathrm{F}}(z, t)\phi(x, y) \tag{18}$$

$$E_{ij} = \bar{E}_{ij} + \hat{E}_{ij}(z, t)\phi(x, y) \tag{19}$$

$$T_{ij} = \bar{T}_{ij} + \hat{T}_{ij}(z, t)\phi(x, y) \tag{20}$$

where $\phi(x, y)$ is given by

$$\phi(x, y) = \exp(\mathrm{i}a_x x + \mathrm{i}a_y y) \tag{21}$$

where a_x and a_y are the disturbance wave numbers in the x- and y-directions, respectively. The bar symbols, $\bar{}$, over h, E_{ij} and T_{ij} represent the basic state solutions of the related quantities. The first term in the right-hand side of equations (15)–(20) represents the basic state solution associated with the quantity presented on the left-hand side. It should be noted particularly that the perturbation is only expanded in the spatial domain since the solution of the film thickness in the basic state is a time dependent function already. However, the perturbation of equation (21) still valid for the static film, i.e. for $V = 0$ in equation (11).

3.3. Perturbed displacement fields

The linear system of partial differential equations for the disturbances is obtained by substituting the perturbed equations (15)–(21) into the governing equations (6)–(9) and then linearizing the disturbance quantities. The resulting equations for the perturbed field are:

$$(1-2\nu)(\partial_z^2 - a^2)\hat{u}_1 + \mathrm{i}a_x(\mathrm{i}a_x\hat{u}_1 + \mathrm{i}a_y\hat{u}_2 + \partial_z\hat{u}_3) = 0 \quad (22)$$

$$(1-2\nu)(\partial_z^2 - a^2)\hat{u}_2 + \mathrm{i}a_y(\mathrm{i}a_x\hat{u}_1 + \mathrm{i}a_y\hat{u}_2 + \partial_z\hat{u}_3) = 0 \quad (23)$$

$$(1-2\nu)(\partial_z^2 - a^2)\hat{u}_3 + \partial_z(\mathrm{i}a_x\hat{u}_1 + \mathrm{i}a_y\hat{u}_2 + \partial_z\hat{u}_3) = 0 \quad (24)$$

where $a = (a_x^2 + a_y^2)^{1/2}$.

The linearized boundary conditions relating to the perturbed quantities are:

$$-\mathrm{i}a_x\hat{h}\bar{T}_{11}^{\mathrm{F}} + \hat{T}_{13}^{\mathrm{F}} = 0 \qquad \text{on } z = \bar{h} \quad (25)$$

$$-\mathrm{i}a_y\hat{h}\bar{T}_{22}^{\mathrm{F}} + \hat{T}_{23}^{\mathrm{F}} = 0 \qquad \text{on } z = \bar{h} \quad (26)$$

$$\hat{T}_{33}^{\mathrm{F}} = 0 \qquad \text{on } z = \bar{h} \quad (27)$$

$$\hat{u}_i^{\mathrm{S}} = \hat{u}_i^{\mathrm{F}} \qquad \text{on } z = 0 \quad \text{for } i = 1, 2, 3 \quad (28)$$

$$\hat{T}_{3i}^{\mathrm{S}} = \hat{T}_{3i}^{\mathrm{F}} \qquad \text{on } z = 0 \quad \text{for } i = 1, 2, 3 \quad (29)$$

$$\hat{u}_i^{\mathrm{S}} = 0 \qquad \text{on } z = -H \quad \text{for } i = 1, 2, 3. \quad (30)$$

Finally, the linearized evolution equation for the film surface is obtained by substituting equations (15)–(21) into (10), i.e.

$$\frac{\partial\hat{h}}{\partial t} = Da^2(\hat{E} - \gamma\hat{K}) \quad (31)$$

where

$$\hat{E} = 2\mu^{\mathrm{F}}E_{33}^0(\hat{E}_{11}^{\mathrm{F}} + \hat{E}_{22}^{\mathrm{F}}) \qquad \text{on } z = \bar{h} \quad (32)$$

and

$$\hat{K} = a^2(\hat{h} - \hat{u}_3^{\mathrm{F}}) \qquad \text{on } z = \bar{h}. \quad (33)$$

The general solution of equations (22)–(24) in the film is:

$$\hat{u}_1^{\mathrm{F}} = \alpha_1\cosh az + \beta_1\sinh az - \left(\frac{\delta_2\mathrm{i}a_x}{a}\right)z\cosh az - \left(\frac{\delta_1\mathrm{i}a_x}{a}\right)z\sinh az \quad (34)$$

$$\hat{u}_2^{\mathrm{F}} = \alpha_2\cosh az + \beta_2\sinh az - \left(\frac{\delta_2\mathrm{i}a_y}{a}\right)z\cosh az - \left(\frac{\delta_1\mathrm{i}a_y}{a}\right)z\sinh az \quad (35)$$

$$\hat{u}_3^{\mathrm{F}} = \alpha_3\cosh az + \beta_3\sinh az - \delta_1 z\cosh az - \delta_2 z\sinh az \quad (36)$$

where

$$\delta_1 = \left[\frac{1}{3-4\nu^{\mathrm{F}}}\right](\mathrm{i}a_x\alpha_1 + \mathrm{i}a_y\alpha_2 + a\beta_3) \quad (37)$$

$$\delta_2 = \left[\frac{1}{3-4\nu^{\mathrm{F}}}\right](\mathrm{i}a_x\beta_1 + \mathrm{i}a_y\beta_2 + a\alpha_3) \quad (38)$$

and the general solution of equations (22)–(24) in the substrate is:

$$\hat{u}_1^{\mathrm{S}} = \alpha_4\cosh az + \beta_4\sinh az - \left(\frac{\delta_4\mathrm{i}a_x}{a}\right)z\cosh az - \left(\frac{\delta_3\mathrm{i}a_x}{a}\right)z\sinh az \quad (39)$$

$$\hat{u}_2^{\mathrm{S}} = \alpha_5\cosh az + \beta_5\sinh az - \left(\frac{\delta_4\mathrm{i}a_y}{a}\right)z\cosh az - \left(\frac{\delta_3\mathrm{i}a_y}{a}\right)z\sinh az \quad (40)$$

$$\hat{u}_3^{\mathrm{S}} = \alpha_6\cosh az + \beta_6\sinh az - \delta_3 z\cosh az - \delta_4 z\sinh az \quad (41)$$

where

$$\delta_3 = \left[\frac{1}{3-4\nu^{\mathrm{S}}}\right](\mathrm{i}a_x\alpha_4 + \mathrm{i}a_y\alpha_5 + a\beta_6) \quad (42)$$

$$\delta_4 = \left[\frac{1}{3-4\nu^{\mathrm{S}}}\right](\mathrm{i}a_x\beta_4 + \mathrm{i}a_y\beta_5 + a\alpha_6). \quad (43)$$

The twelve unknown constants, i.e. α_i and β_i ($i = 1, 2, 3, 4, 5, 6$), are solved by incorporating the boundary conditions given in equations (25)–(30). The twelve unknowns will then be expressed in terms of $\hat{h}$. After eliminating the dependent unknown constants by incorporating these boundary conditions, two final independent equations, in terms of δ_1 and δ_2, are obtained as,

$$\Lambda_1\delta_1 + \Omega_1\delta_2 = \Pi_1 \quad (44)$$

$$\Lambda_2\delta_1 + \Omega_2\delta_2 = \Pi_2. \quad (45)$$

Finally, expressions for δ_1 and δ_2 are obtained using Cramer's rule, i.e.

$$\delta_1 = \frac{\Pi_1\Omega_2 - \Pi_2\Omega_1}{\Delta} = \hat{h}\left(\frac{\Delta_1}{\Delta}\right) \quad (46)$$

$$\delta_2 = \frac{\Lambda_1\Pi_2 - \Lambda_2\Pi_1}{\Delta} = \hat{h}\left(\frac{\Delta_2}{\Delta}\right). \quad (47)$$

The expressions for Λ_1, Ω_1, Π_1, Λ_2, Ω_2 and Π_2 are presented in equations (A1)–(A6), while the expressions for Δ, Δ_1 and Δ_2 are given in equations (A7)–(A9). It is noted that the parameter ρ, defined in equations (A1)–(A9), is an important parameter, which measures the relative stiffness of the film to that of the substrate, i.e. $\rho = \mu^{\mathrm{F}}/\mu^{\mathrm{S}}$, that will be referred in the following section.

Once δ_1 and δ_2 have been solved, the elastic states of the film and the substrate can be determined. Expressions for $\hat{E}_{11}^{\mathrm{F}}$ and $\hat{E}_{22}^{\mathrm{F}}$, given in equation (32), are presented in equations (A10)–(A13). Therefore, the perturbed evolution equation can be expressed as follows:

$$\frac{\partial\hat{h}}{\partial t} = \hat{h}\sigma \quad (48)$$

where

$$\sigma = D\{a^3 E_0 F(a\bar{h}, aH) - a^4\gamma[1 - K_0 G(a\bar{h}, aH)]\} \quad (49)$$

$$E_0 = 4\mu^{\mathrm{F}}(1-\nu^{\mathrm{F}})(E_{33}^0)^2 = 4\varepsilon^2\mu^{\mathrm{F}}\left[\frac{(1+\nu^{\mathrm{F}})^2}{1-\nu^{\mathrm{F}}}\right] \quad (50)$$

$$K_0 = E_{33}^0 = \varepsilon\left[\frac{1+\nu^{\mathrm{F}}}{1-\nu^{\mathrm{F}}}\right]. \quad (51)$$

The expressions for $F(a\bar{h}, aH)$ and $G(a\bar{h}, aH)$ are shown in equations (A14) and (A15).

4. Results and discussion

The parameters used in the numerical calculation are listed in table 1, and are the same as those presented previously in [6]. The parameters that are not presented in table 1, for example, ρ, $a\bar{h}$, and aH, are the variable dimensionless parameters whose effects upon the stability characteristics are investigated in the current study.

Figure 2 shows the relationship between the normal-mode growth rate, σ, and the wave numbers, a, as derived from equation (48). The curve determines the stability characteristics of the static film. As may be seen in equation (49), σ is represented by the subtraction of two terms, and may be regarded to be the net result of two competing energies, namely strain energy, which is proportional to a^3, and surface energy, which is proportional to a^4. The results shown in figure 2 indicate that strain energy tends to destabilize the system, while surface energy has the opposite effect providing that $K_0 G(a\bar{h}, aH) < 1$. As may be surmised from equation (51), this term is usually quite small, since K_0 is small. The unstable region ($\sigma > 0$) is evident for small wave numbers, and belongs to the category of long wave instability, while the stable region ($\sigma < 0$) occurs for large wave numbers, belonging to the short wave stability. The intersection of the curve σ and the axis of the wave number represents the critical wave number, a_{c} ($\sigma = 0$).

The dimensional characteristic length l ($= \gamma/E_0$) is defined as the ratio of the surface energy density, γ, to the basic-state strain energy density, E_0. The dimensionless wave number is defined as $a_{\mathrm{c}}l$, the dimensionless film thickness is defined as h_0/l, and the dimensionless substrate thickness is defined as H/l. In order to verify the validity of the results formulated in this study, the solution from equation (49) is reduced to the case of an infinite substrate thickness, and the results are then compared to those provided by Spencer *et al* [6]. As shown in figure 3, there is excellent agreement between the two sets of results.

The discussion which follows considers the results obtained for values of stiffness ratio greater than, equal to and less than unity. Figure 4 shows the relationship between the dimensionless wave number ($a_{\mathrm{c}}l$) and the dimensionless film thickness (h_0/l) for different dimensionless substrate thicknesses in the case of a stiffness ratio of $\rho = 2$. (Note that in the remaining discussions, the relationship between the dimensionless wave number and the dimensionless film thickness will be referred to as the $a_{\mathrm{c}}l$–h_0/l.) The results indicate that the stable region decreases as the substrate thickness increases. In general, the influence of the substrate–holder interface condition (i.e. zero displacement) is to stabilize the system, since this condition tends to restrict the motion of the substrate relative to the motion of the film. Note that although the magnitude of the misfitting strain is independent of the substrate thickness, the degree of restriction imposed on the motion of the film does depend upon the substrate thickness. It is found that the degree of constraint on the film motion increases as the substrate thickness, or, to express this in another way, the stable region decreases as the substrate thickness increases. For a given substrate

Table 1. Parameters for epitaxially strained films on a substrate with finite thickness [6].

Parameter	Value
ε	0.0418
γ	$1.927 \times 10^{-3}\ \mathrm{J\,m^{-2}}$
ν^{F}	$\frac{1}{3}$
ν^{S}	$\frac{1}{3}$
μ^{F}	$5.68 \times 10^{10}\ \mathrm{J\,m^{-3}}$

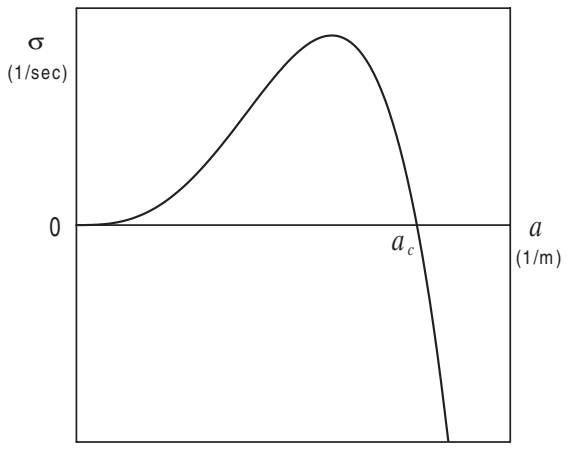

Figure 2. Typical plot of the normal-mode growth rate, σ, versus the wave number, a.

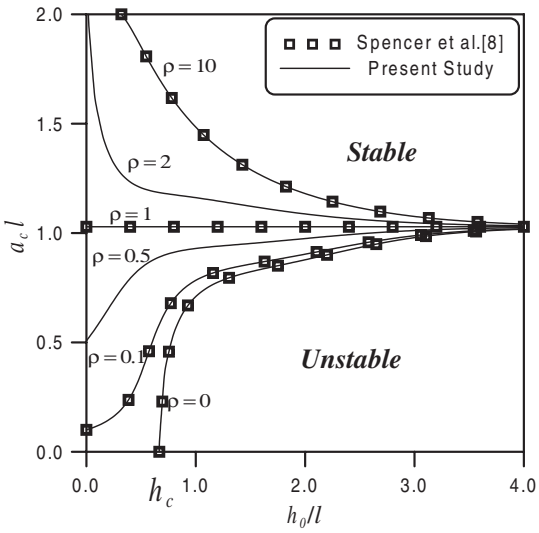

Figure 3. The dimensional wave number, $a_{\mathrm{c}}l$, versus the dimensional film thickness, h_0/l, for the case of the substrate thickness approaching infinity, $H \to \infty$.

thickness, the system generally becomes more stable as the film thickness increases, other than for smaller substrate thicknesses. Furthermore, it can be seen that the stability of the system is not influenced by the film thickness when the dimensionless film thickness exceeds a value of 4. It will also be noted that there is a wide variation of the neutral curves in the region where the film thickness is close to h_c. The results presented in figure 4 indicate that the effects of finite substrate thickness are significant, particularly when the film thickness is close to h_c, and that for a stiffer film ($\rho > 1$), the system becomes more stable as the film thickness increases.

Figure 5 shows the $a_c l$–h_0/l relationship for a stiffness ratio of $\rho = 1$ in the case of homoepitaxial film growth. The influence of the substrate thickness on the stability characteristics of the system is similar to that reported previously in figure 4. Compared to figure 4, it will be noted that the system becomes more unstable as the film thickness increases, i.e. the reverse of the results observed for a stiffness ratio of $\rho = 2$. The chief constraint in this particular system comes from the substrate–holder interface condition since in a homoepitaxial case the same material is used in both the film and the substrate. Therefore, as the film thickness increases the constraint becomes weaker, and this results in a destabilizing of the system.

Figure 6 shows the $a_c l$–h_0/l relationship for a stiffness ratio of $\rho = 0.5$. The results are similar to those presented in figure 5. It is noted that for a softer film ($\rho < 1$), the system becomes more unstable as the film thickness increases.

Figure 7 shows the $a_c l$–h_0/l relationship for the case of a rigid substrate, i.e. $\rho = 0$. The results indicate that the substrate thickness has no influence on the stability characteristics when the substrate is rigid. The physical explanation for this might be that since the substrate is perfectly rigid ($\rho = 0$), any disturbance mode only influences the film and has no effect on the substrate. Thus, for any

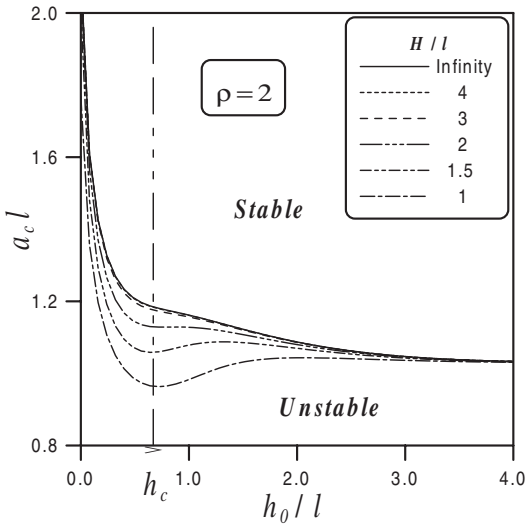

Figure 4. The dimensional wave number, $a_c l$, versus the dimensional film thickness, h_0/l, for the case of the stiffness ratio, $\rho = 2$.

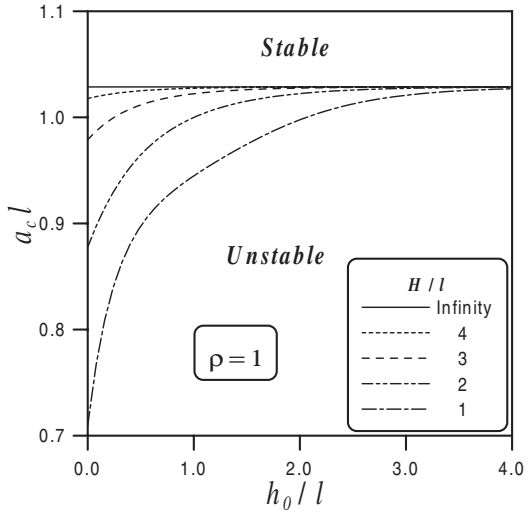

Figure 5. The dimensional wave number, $a_c l$, versus the dimensional film thickness, h_0/l, for the case of the stiffness ratio, $\rho = 1$.

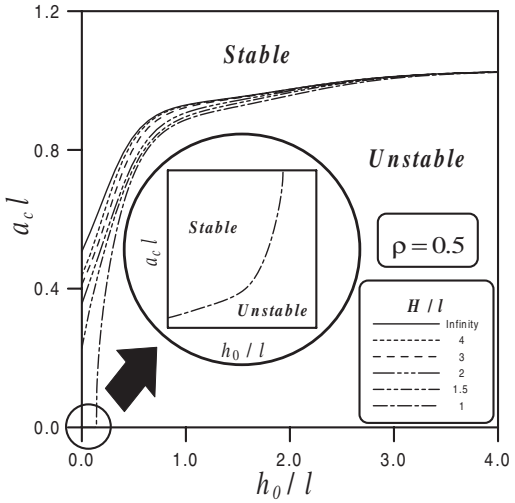

Figure 6. The dimensional wave number, $a_c l$, versus the dimensional film thickness, h_0/l, for the case of the stiffness ratio, $\rho = 0.5$.

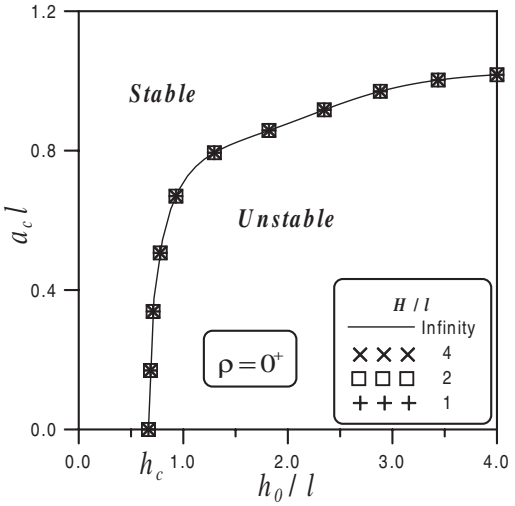

Figure 7. The dimensional wave number, $a_c l$, versus the dimensional film thickness, h_0/l, for the case of the stiffness ratio, $\rho = 0^+$.

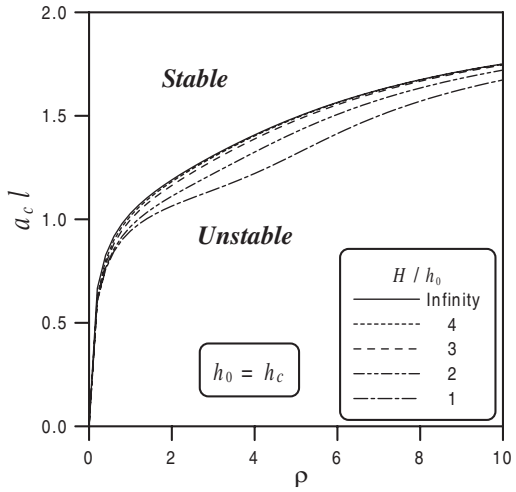

Figure 8. The dimensional wave number, $a_c l$, versus the stiffness ratio, ρ, for the case of the basic state solution of film thickness equal to the critical film thickness, i.e. $h_0 = h_c$.

substrate thickness, the critical height remains unchanged if an assumption is made that the substrate is perfectly rigid. In addition, it can be seen that there exists an absolutely stable region when the film thickness is smaller than the critical film thickness, h_c. The value of h_c is equal to $A_F l/2$, and is evaluated by L'Hôspital's rule.

Figure 8 shows the dimensionless wave number versus the dimensionless stiffness ratio for different dimensionless substrate thicknesses, in the case where the fixed film thickness is equal to h_c. The results indicate that the system becomes more unstable as the dimensionless stiffness ratio increases, i.e. the system becomes more unstable for softer substrates (ρ is larger).

5. Conclusions

This paper has investigated the morphological stability of epitaxial films growing heteroepitaxially on ultra-thin substrates. A finite substrate thickness has been included in the physical model in order to derive the effects of substrate thickness on the stability characteristics of the system. This reflects the gradual decrease in substrate thickness used in practice. The results presented below, which summarize the principal conclusions of the current investigation, focus on the influence of the finite substrate thickness effect on the stability characteristics of the strained film, and therefore represent findings which are not obtained when considering the infinite substrate thickness addressed by Spencer *et al* [6].

(1) Decreasing the substrate thickness or increasing the substrate stiffness has a stabilizing effect on the system.
(2) The effect on the system stability as the substrate thickness is increased tends to be similar regardless of whether the stiffness ratio of the film to the substrate is less than, equal to, or greater than unity. The system tends to stabilize in all cases.
(3) For a specific substrate thickness, increasing the film thickness has a destabilizing effect upon the system, apart from the case of smaller substrate thicknesses with a stiffness ratio larger than unity. This result is similar to that obtained for the infinite substrate thickness.
(4) A finite substrate thickness has no influence on the stability behaviour of the system when a perfectly rigid substrate is considered.
(5) The effect of a finite thickness substrate on the stability behaviour of the system is significant when the stiffness ratio is larger than unity, especially when the film thickness is close to h_c. However, a finite substrate thickness has no effect upon the stability behaviour when the dimensionless film thickness is larger than 4, regardless of the value of the stiffness ratio.

It is noted that the conclusions provided above are based on the assumption of a rigid holder. It is acknowledged that this assumption may not truly reflect the case of a deformable holder which might be encountered in practice. However, this assumption is adopted in order to simplify the complicated three-layer model required for a deformable substrate to a two-layer model. This significantly reduces the computational effort required to derive an analytical solution. It is recognized that the results of the simplified two-layer model are not as accurate as those of the three-layer model. However, the results nevertheless provide an initial approximation of the film evolution problem with a finite thickness substrate in most cases, and this provides a preliminary understanding of the stability characteristics of the film. The more accurate solution of a three-layer model would involve the simultaneous solution of three sets of governing equations associated with the solid–solid and solid–vapour interfaces. This would greatly complicate the analytical solution of the problem. An alternative future approach would be to employ a semi-analytical and numerical method to solve the problem.

Acknowledgments

The current authors wish to express their thanks to Professor Cheng-I Weng for his assistance during the physical modelling stage of this study and for his help in related discussions. Furthermore, the authors would like to acknowledge the support afforded to this study by the National Science Council of the Republic of China under Contract No NSC 91-2212-E006-165.

Appendix

$$\begin{aligned}\Lambda_1 = {} & [A_S(a\bar{h}) + (B_F + \rho)(aH) + A_S \cosh a\bar{h} \sinh a\bar{h} \\ & + (1-\rho)(aH)\cosh^2 a\bar{h} \\ & - (B_F + \rho)C_S \cosh aH \sinh aH \\ & + (1-\rho)C_S(a\bar{h})\sinh^2 aH \\ & - (1-\rho)C_S \cosh^2 a\bar{h} \cosh aH \sinh aH \\ & + (1-\rho)C_S \cosh a\bar{h} \sinh a\bar{h} \sinh^2 aH] \end{aligned} \tag{A1}$$

$$\begin{aligned}\Omega_1 = {} & [A_F A_S - (1-\rho)(a\bar{h})(aH) + A_S \sinh^2 a\bar{h} \\ & + (1-\rho)(aH)\cosh a\bar{h} \sinh a\bar{h} + A_F C_S \sinh^2 aH \\ & + (1-\rho)C_S(a\bar{h})\cosh aH \sinh aH \\ & + (1-\rho)C_S \sinh^2 a\bar{h} \sinh^2 aH \\ & - (1-\rho)C_S \cosh a\bar{h} \sinh a\bar{h} \cosh aH \sinh aH] \end{aligned} \tag{A2}$$

$$\begin{aligned}\Pi_1 = {} & aE_{33}^0 \hat{h}[A_S \cosh a\bar{h} + (1-\rho)(aH)\sinh a\bar{h} \\ & - (1-\rho)C_S \sinh a\bar{h} \cosh aH \sinh aH \\ & + (1-\rho)C_S \cosh a\bar{h} \sinh^2 aH] \end{aligned} \tag{A3}$$

$$\begin{aligned}\Lambda_2 = [&B_F A_S - (1-\rho)(a\bar{h})(aH) + A_S \cosh^2 a\bar{h} \\ &+ (B_F + \rho) C_S \sinh^2 aH \\ &- (1-\rho)(aH)\cosh a\bar{h} \sinh a\bar{h} \\ &- (1-\rho) C_S (a\bar{h}) \cosh aH \sinh aH \\ &+ (1-\rho) C_S \cosh^2 a\bar{h} \sinh^2 aH \\ &- (1-\rho) C_S \cosh a\bar{h} \sinh a\bar{h} \cosh aH \sinh aH] \end{aligned} \tag{A4}$$

$$\begin{aligned}\Omega_2 = [&-A_S(a\bar{h}) - A_F(aH) + A_S \cosh a\bar{h} \sinh a\bar{h} \\ &- (1-\rho) aH \sinh^2 a\bar{h} - A_F C_S \cosh aH \sinh aH \\ &- (1-\rho) C_S (a\bar{h}) \sinh^2 aH \\ &- (1-\rho) C_S \sinh^2 a\bar{h} \cosh aH \sinh aH \\ &+ (1-\rho) C_S \cosh a\bar{h} \sinh a\bar{h} \sinh^2 aH] \end{aligned} \tag{A5}$$

$$\begin{aligned}\Pi_2 = a E^0_{33} \hat{h} [&A_S \sinh a\bar{h} - (1-\rho)(aH)\cosh a\bar{h} \\ &- (1-\rho) C_S \cosh a\bar{h} \cosh aH \sinh aH \\ &+ (1-\rho) C_S \sinh a\bar{h} \sinh^2 aH] \end{aligned} \tag{A6}$$

$$\begin{aligned}\Delta = &(\Lambda_1 \Omega_2 - \Lambda_2 \Omega_1) \\ = &-(2[A_F + B_F C_F + 2(a\bar{h})^2][A_S + B_S C_S + 2(aH)^2] \\ &+ 4\rho\{4 A_F A_S (a\bar{h})(aH) \\ &+ [B_F - 2(a\bar{h})^2][B_S C_S + 2(aH)^2]\} \\ &+ 2\rho^2 [1 + 2(a\bar{h})^2][C_S^2 + 2(aH)^2] + 2[C_F(A_S + B_S C_S) \\ &- 2\rho B_F B_S C_S - \rho^2 C_S^2 \\ &+ 2(1-\rho)(\rho + C_F)(aH)^2]\cosh 2a\bar{h} \\ &+ 2C_S[(A_F + B_F C_F) - 2\rho B_F B_S - \rho^2 C_S \\ &+ 2(1-\rho)(1+\rho C_S)(a\bar{h})^2]\cosh 2aH \\ &+ C_S(1-\rho)(C_F - \rho C_S)\cosh 2a(\bar{h} - H) \\ &+ C_S(\rho + C_F)(1+\rho C_S)\cosh 2a(\bar{h} + H))/8 \end{aligned} \tag{A7}$$

$$\begin{aligned}\Delta_1 = &-a E^0_{33}(4\rho A_F A_S (aH)\cosh a\bar{h} \\ &+ 2[A_S + B_S C_S - 2\rho B_S C_S + \rho^2 C_S^2 \\ &+ 2(1-\rho)^2 (aH)^2](a\bar{h})\cosh a\bar{h} \\ &+ 2C_S(1-\rho)(1+\rho C_S)(a\bar{h})\cosh a\bar{h}\cosh 2aH \\ &+ 2[B_F(A_S + B_S C_S) + 2\rho\nu_F B_S C_S - \rho^2 C_S^2 \\ &+ 2(1-\rho)(\rho + B_F)(aH)^2]\sinh a\bar{h} \\ &+ C_S(1-\rho)(B_F - \rho C_S)\sinh a(\bar{h} - 2H) \\ &+ C_S(\rho + B_F)(1+\rho C_S)\sinh a(\bar{h} + 2H))/4 \end{aligned} \tag{A8}$$

$$\begin{aligned}\Delta_2 = &-a E^0_{33}(-2A_F[(3\rho - 5) - 2\nu_S(5\rho - 6) \\ &- 8\nu_S^2(1-\rho) - 2(1-\rho)(aH)^2]\cosh a\bar{h} \\ &- 2a\{2A_F A_S \rho H + \bar{h}[(5 - 6\rho) - 4\nu_S(2 + B_S) \\ &+ 4\rho\nu_S(2 + C_S) + \rho^2 C_S^2 + 2(1-\rho)^2 (aH)^2]\}\sinh a\bar{h} \\ &+ A_F C_S (1-\rho)\cosh a(\bar{h} - 2H) \\ &+ A_F C_S (1+\rho C_S)\cosh a(\bar{h} + 2H) \\ &- C_S(1-\rho)(1+\rho C_S)(a\bar{h})\sinh a(\bar{h} - 2H) \\ &- C_S(1-\rho)(1+\rho C_S)(a\bar{h})\sinh a(\bar{h} + 2H))/4 \end{aligned} \tag{A9}$$

where ρ is the stiffness ratio, i.e. $\rho = \mu^F/\mu^S$, which is an important elastic parameter measuring the relative stiffness of the film to that of the substrate. In addition, $A = 2(1-\nu)$, $B = 1 - 2\nu$ and $C = 3 - 4\nu$. The subscripts F and S for A, B and C refer to the film and to the substrate, respectively.

$$\begin{aligned}\hat{E}^F_{11} &= \mathrm{i} a_x \hat{u}^F_1 \\ &= \left(\frac{a_x}{a}\right)^2 [(C_F\delta_1 - a\beta_3)\cosh a\bar{h} + (C_F\delta_2 - a\alpha_3)\sinh a\bar{h} \\ &\quad + \delta_2(a\bar{h})\cosh a\bar{h} + \delta_1(a\bar{h})\sinh a\bar{h}] \\ &= \left(\frac{a_x}{a}\right)^2 \left(\frac{\hat{h}}{\Delta}\right)[(C_F\Delta_1 - B_3)\cosh a\bar{h} \\ &\quad + (C_F\Delta_2 - A_3)\sinh a\bar{h} + \Delta_2(a\bar{h})\cosh a\bar{h} \\ &\quad + \Delta_1(a\bar{h})\sinh a\bar{h}] \end{aligned} \tag{A10}$$

$$\begin{aligned}\hat{E}^F_{22} &= \mathrm{i} a_y \hat{u}^F_2 \\ &= \left(\frac{a_y}{a}\right)^2 [(C_F\delta_1 - a\beta_3)\cosh a\bar{h} + (C_F\delta_2 - a\alpha_3)\sinh a\bar{h} \\ &\quad + \delta_2(a\bar{h})\cosh a\bar{h} + \delta_1(a\bar{h})\sinh a\bar{h}] \\ &= \left(\frac{a_y}{a}\right)^2 \left(\frac{\hat{h}}{\Delta}\right)[(C_F\Delta_1 - B_3)\cosh a\bar{h} \\ &\quad + (C_F\Delta_2 - A_3)\sinh a\bar{h} \\ &\quad + \Delta_2(a\bar{h})\cosh a\bar{h} + \Delta_1(a\bar{h})\sinh a\bar{h}] \end{aligned} \tag{A11}$$

where A_3 and B_3 are,

$$\begin{aligned}A_3 = [&(a\bar{h} + \cosh a\bar{h}\sinh a\bar{h})\Delta_1 + (A_F + \sinh^2 a\bar{h})\Delta_2 \\ &- a E^0_{33}\Delta\cosh a\bar{h}] \end{aligned} \tag{A12}$$

$$\begin{aligned}B_3 = [&-(-A_F + \cosh^2 a\bar{h})\Delta_1 - (-a\bar{h} + \cosh a\bar{h}\sinh a\bar{h})\Delta_2 \\ &+ a E^0_{33}\Delta\sinh a\bar{h}] \end{aligned} \tag{A13}$$

$$\begin{aligned}F(a\bar{h}, aH) &= [(C_F\Delta_1 - B_3)\cosh a\bar{h} + (C_F\Delta_2 - A_3)\sinh a\bar{h} \\ &\quad + \Delta_2(a\bar{h})\cosh a\bar{h} + \Delta_1(a\bar{h})\sinh a\bar{h}] \\ &\quad \times [2a(1+\nu_F)\Delta E^0_{33}]^{-1} \\ &= -(4\{(a\bar{h})[A_S + B_S C_S + 2(aH)^2] \\ &\quad + 2\rho[-B_S C_S(a\bar{h}) + A_F A_S(aH) - 2(a\bar{h})(aH)^2] \\ &\quad + \rho^2(a\bar{h})[C_S^2 + 2(aH)^2]\} + 2\{C_F[A_S + B_S C_S + 2(aH)^2] \\ &\quad - 2\rho B_F[B_S C_S + 2(aH)^2] - \rho^2[C_S^2 + 2(aH)^2]\}\sinh 2a\bar{h} \\ &\quad + 4C_S(1-\rho)(1+\rho C_S)(a\bar{h})\cosh 2aH \\ &\quad + C_S(C_F + \rho)(1+\rho C_S)\sinh 2a(\bar{h} + H) \\ &\quad + C_S(1-\rho)(C_F - \rho C_S)\sinh 2a(\bar{h} - H))/8\Delta \end{aligned} \tag{A14}$$

$$\begin{aligned}G(a\bar{h}, aH) &= [\mathrm{A}_3\cosh a\bar{h} + \mathrm{B}_3\sinh a\bar{h} \\ &\quad - \Delta_1(a\bar{h})\cosh a\bar{h} - \Delta_2(a\bar{h})\sinh a\bar{h}][a\Delta E^0_{33}]^{-1} \\ &= -(2[B_F C_F + 2(a\bar{h})^2][A_S + B_S C_S + 2(aH)^2] \\ &\quad - 4\rho\{[C_F - 2(a\bar{h})^2][B_S C_S + 2(aH)^2] \\ &\quad + 4A_F A_S(a\bar{h})(aH)\} \\ &\quad + 2\rho^2[B_F - 2(a\bar{h})^2][C_S^2 + 2(aH)^2] \\ &\quad + 2B_F[2(1-\rho)(C_F + \rho)(aH)^2 + C_F(A_S + B_S C_S) \\ &\quad - 2\rho B_F B_S C_S - \rho^2 C_S^2]\cosh 2a\bar{h} \\ &\quad - 2C_S[2(1-\rho)(1+\rho C_S)(a\bar{h})^2 + B_F C_F - 2\rho C_F B_S \\ &\quad + \rho^2 B_F C_S]\cosh 2aH \\ &\quad + B_F C_S(C_F + \rho)(1+\rho C_S)\cosh 2a(\bar{h} + H) \\ &\quad + B_F C_S(1-\rho)(C_F - \rho C_S)\cosh 2a(\bar{h} - H))/8\Delta. \end{aligned} \tag{A15}$$

References

[1] Pinel S, Tasselli J, Bailbé J P, Marty A, Puech P and Estéve D 2000 Mechanical lapping of ultra-thin wafers for 3D integration *Proc. 22nd Int. Conf. on Microelectronics* vol 2, pp 443–6

[2] Sriram S and Smith T J Jr 2000 Reduction of common-source inductance in FET/HEMT structures utilizing wave-propagation effects *IEEE Trans. Microwave Theory Technol.* **48** 406–11

[3] Yakovlev A B, Khalil A I and Hicks C W 2000 The generalized scattering matrix of closely spaced strip and slot layers in waveguide *IEEE Trans. Microwave Theory Technol.* **48** 126–37

[4] Ma E Y, Theiss S D, Lu M H, Wu C C, Sturm J C and Wagner S 1997 Thin film transistors for foldable displays *Electron Devices Meeting, Tech. Dig. Int.* pp 535–8

[5] Grief M K and Steele J A Jr 1996 Warpage and mechanical strength studies of ultra thin 150 mm wafers *Electron. Manuf. Technol. Symp., 19th IEEE/CPMT* pp 190–4

[6] Spencer B J, Voorhees P W and Davis S H 1991 Morphological instability in epitaxially strained dislocation-free solid films *Phys. Rev. Lett.* **67** 3696–9

[7] Spencer B J, Voorhees P W and Davis S H 1993 Morphological instability in epitaxially strained dislocation-free solid films: linear stability theory *J. Appl. Phys.* **73** 4955–70

[8] Spencer B J 1992 Morphological instability and the effect of elastic stresses *PhD Dissertation* Northwestern University

[9] Asaro R J and Tiller W A 1972 Interface morphology development during stress corrosion cracking: Part I. Via surface diffusion *Metall. Trans.* **3** 1789–96

[10] Srolovitz D J 1989 On the stability of surfaces of stressed solids *Acta Metall. Mater.* **37** 621–5

[11] Grinfel'd M A 1986 Instability of the separation boundary between a non-hydrostatically stressed elastic body and a melt *Sov. Phys.—Dokl.* **31** 831–4

[12] Junqua N and Grilhé J 1993 Surface instability of epitaxially films on a substrate *J. Phys. III (France)* **3** 1589–601

[13] Gao H 1994 Some general properties of stress-driven surface evolution in a heteroepitaxial thin film structure *J. Mech. Phys. Solids* **42** 741–72